Cerebral Microbleeds: Imaging and Clinical Significance[1]

Sven Haller, MD, MSc
Meike W. Vernooij, MD, PhD
Joost P. A. Kuijer, PhD
Elna-Marie Larsson, MD, PhD
Hans Rolf Jäger, MD, FRCR
Frederik Barkhof, MD, PhD

Cerebral microbleeds (CMBs), also referred to as microhemorrhages, appear on magnetic resonance (MR) images as hypointense foci notably at T2*-weighted or susceptibility-weighted (SW) imaging. CMBs are detected with increasing frequency because of the more widespread use of high magnetic field strength and of newer dedicated MR imaging techniques such as three-dimensional gradient-echo T2*-weighted and SW imaging. The imaging appearance of CMBs is mainly because of changes in local magnetic susceptibility and reflects the pathologic iron accumulation, most often in perivascular macrophages, because of vasculopathy. CMBs are depicted with a true-positive rate of 48%–89% at 1.5 T or 3.0 T and T2*-weighted or SW imaging across a wide range of diseases. False-positive "mimics" of CMBs occur at a rate of 11%–24% and include microdissections, microaneurysms, and microcalcifications; the latter can be differentiated by using phase images. Compared with postmortem histopathologic analysis, at least half of CMBs are missed with premortem clinical MR imaging. In general, CMB detection rate increases with field strength, with the use of three-dimensional sequences, and with postprocessing methods that use local perturbations of the MR phase to enhance T2* contrast. Because of the more widespread availability of high-field-strength MR imaging systems and growing use of SW imaging, CMBs are increasingly recognized in normal aging, and are even more common in various disorders such as Alzheimer dementia, cerebral amyloid angiopathy, stroke, and trauma. Rare causes include endocarditis, cerebral autosomal dominant arteriopathy with subcortical infarcts, leukoencephalopathy, and radiation therapy. The presence of CMBs in patients with stroke is increasingly recognized as a marker of worse outcome. Finally, guidelines for adjustment of anticoagulant therapy in patients with CMBs are under development.

Online SA-CME
See www.rsna.org/education/search/ry

Learning Objectives:
After reading the article and taking the test, the reader will be able to:

- Describe how technical MR parameters and sequence protocols may influence the detection of cerebral microbleeds (CMBs)
- Discuss limitations of the detection of CMBs in MR imaging and how to distinguish CMBs from microbleed mimics
- Discuss the role of increasing microbleed accumulation during aging and cognitive decline
- Explain how the spatial distribution of CMBs may contribute to differential diagnosis

Accreditation and Designation Statement
The RSNA is accredited by the Accreditation Council for Continuing Medical Education (ACCME) to provide continuing medical education for physicians. The RSNA designates this journal-based SA-CME activity for a maximum of 1.0 *AMA PRA Category 1 Credit*™. Physicians should claim only the credit commensurate with the extent of their participation in the activity.

Disclosure Statement
The ACCME requires that the RSNA, as an accredited provider of CME, obtain signed disclosure statements from the authors, editors, and reviewers for this activity. For this journal-based CME activity, author disclosures are listed at the end of this article.

[1] From the Affidea Centre de Diagnostic Radiologique de Carouge (CDRC), Geneva, Switzerland (S.H.); Faculty of Medicine, University of Geneva, Geneva, Switzerland (S.H.); Department of Surgical Sciences, Radiology, Uppsala University, Uppsala, Sweden (S.H., E.M.L.); Department of Neuroradiology, University Hospital Freiburg, Freiburg, Germany (S.H.); Department of Radiology and Nuclear Medicine and Department of Epidemiology, Erasmus Medical Center, Rotterdam, the Netherlands (M.W.V.); Department of Radiology and Nuclear Medicine, Amsterdam Neuroscience, VU University Medical Center, Amsterdam, the Netherlands (J.P.A.K., F.B.); Neuroradiological Academic Unit, Department of Brain Repair and Rehabilitation, Institute of Neurology, University College London, London, England (H.R.J., F.B.). Received April 5, 2017; revision requested May 22; revision received June 20; accepted July 14; final version accepted July 28. **Address correspondence to** S.H. (e-mail: *sven.haller@gmail.com*).

Cerebral microbleeds (CMBs), also referred to as cerebral microhemorrhages, are small hypointense foci with a maximum size up to 5 mm or even 10 mm detected by using susceptibility-weighted (SW) magnetic resonance (MR) imaging (1–5). Histopathologically, CMBs represent focal accumulations of hemosiderin-containing macrophages (6) with paramagnetic properties causing signal loss because of susceptibility effects. Because of the increasing use of high-field-strength MR imaging systems and dedicated imaging sequences—notably, three-dimensional T2*-weighted imaging, SW imaging, and related techniques—CMBs are increasingly depicted during MR imaging of the brain. CMBs may be observed as an incidental finding or in the context of a specific pathologic finding such as cerebral amyloid angiopathy (CAA). Despite the increased detection rate, clear guidance for radiologists for the interpretation of CMBs are currently lacking and their clinical significance remains controversial.

The sensitivity of MR imaging to depict microbleeds depends on technical aspects, for example, field strength and pulse-sequence parameters. To allow correct depiction of CMBs, we first discuss the optimal MR imaging technique. Once a potential CMB is observed, correct classification requires knowledge about pathologic correlations and potential CMB "mimics," which we address in the next section. Then, we review the interpretation of CMBs in various clinical situations and diseases, such as aging, dementia, radiation therapy, and traumatic brain injury. Finally, we discuss the clinical significance of CMBs in stroke and the clinical management of CMBs.

Essentials

- Currently, even optimized MR imaging sequences at 1.5 T and 3.0 T depict only about 50% of cerebral microbleeds (CMBs).
- CMB "mimics" (false-positive findings) include microdissections, microaneurysms, and microcalcifications.
- The spatial distribution of CMBs contains diagnostic information, for example, lobar distribution typical in cerebral amyloid angiopathy and more diffuse (including deep or central) distribution typical for hypertensive CMBs; a larger number of CMBs is associated with higher risk of cognitive decline, dementia, and stroke.
- Microbleeds in mild traumatic brain injury, also known as hemorrhagic diffuse axonal injury in this context, typically have a linear and radial distribution (in contrast to typical spherical CMBs) and provide a sensitive and persistent imaging marker.

MR Imaging of CMBs: Technical Considerations

Effect of Magnetic Field Strength

Susceptibility effects scale linearly with field strength; hence, the detection rate of CMB at MR imaging increases markedly even between 1.5 T and 3.0 T (7,8). At ultra high field strength (7.0 T and above), sensitivity increases even further (9–11). One study reported CMBs in up to 44% of healthy control participants and in 78% of patients with Alzheimer dementia (AD) at 7.0 T (12). This finding indicates that CMB detection rates at clinical field strengths (1.5 T and 3.0 T) only represent the so-called tip of the iceberg.

Gradient-echo T2*-weighted Imaging, SW Imaging, and Related Techniques

Conventional T2*-weighed contrast can be generated by using a gradient-echo (GRE) pulse sequence, where the echo time determines the amount of contrast. Typically, echo times of 20–60 msec at 1.5 T and 15–40 msec at 3.0 T would be regarded as suitable for T2*-weighted imaging. In conventional T2*-weighted pulse sequences, a CMB appears as a small area of signal loss on the magnitude image. The signal loss results from intravoxel dephasing because of local perturbation of the main magnetic field, in turn caused by high concentrations of iron. Multiple pulse-sequence parameters including two-dimensional and three-dimensional acquisition, echo time, voxel size, and notably field strength influence the image contrast and consequently the detection rate of CMBs on T2*-weighed images.

We refer to SW imaging (13) as a combination of acquisition and postprocessing targeted at enhancing the susceptibility contrast. SW imaging typically employs three-dimensional high-spatial-resolution fully flow-compensated GRE imaging with prolonged echo times. Postprocessing of SW imaging involves multiplication of magnitude images with high-pass filtered phase images (14) to enhance depiction of hemosiderin deposits. In general, phase information facilitates distinction of CMBs from mimics such as calcification (discussed in more detail in the next section). SW imaging permits better depiction of CMBs compared with two-dimensional GRE sequences (2,7,15). For example, in mild cognitive impairment, the detection rate increases from around 20% on routine two-dimensional T2*-weighted GRE images to around 40% on SW images at 3.0 T (2,3,16).

Compared with conventional two-dimensional GRE imaging, the increased detection rate of SW imaging (Fig 1) comes at the cost of longer scan duration associated with high-spatial-resolution three-dimensional imaging. Fast imaging techniques such as parallel imaging, and in the near future possibly compressed sensing, can keep scan times under 5 minutes. An interesting methodologic compromise is to

https://doi.org/10.1148/radiol.2018170803

Content code: NR

Radiology 2018; 287:11–28

Abbreviations:
AD = Alzheimer dementia
CAA = cerebral amyloid angiopathy
CMB = cerebral microbleed
GRE = gradient echo
QSM = quantitative susceptibility mapping
SW = susceptibility weighted

Conflicts of interest are listed at the end of this article.

Figure 1

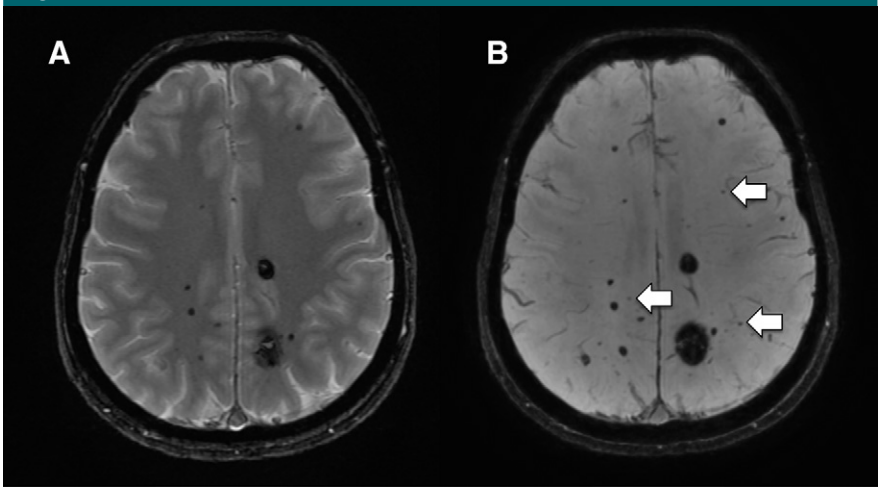

Figure 1: Images in a 53-year-old woman with familial cavernomatosis and multiple cavernomas of variable size. Larger-size cavernomas are well visualized on both, *A,* two-dimensional T2*-weighted and, *B,* three-dimensional multiecho T2*-weighted images. In particular, smaller-sized lesions are better visualized or only visible on three-dimensional multiecho T2*-weighted image (arrows).

perform SW imaging postprocessing of two-dimensional GRE T2*-weighted data to improve susceptibility contrast without increasing scan time (17).

Microbleeds versus Microcalcifications: Magnitude and Phase Images

Not every black dot on susceptibility images constitutes a CMB, and small foci of calcification may mimic CMBs on SW imaging sequences (Fig 2). This differentiation is usually simple at computed tomography (CT) because calcifications are hyperdense, yet CT scans are not always available and small calcifications may not be depicted at CT. For MR imaging, phase images may also discriminate microbleeds from calcifications because calcium is diamagnetic and iron paramagnetic with opposing phase shifts (18). Consequently, CMBs may appear either hyperintense or hypointense on phase maps in different MR systems, depending on whether the imager uses a right- or left-handed coordinate system (19). Phase images are an inherent part of all MR sequences and need no additional imaging time, yet these images are typically not saved by default. Saving phase images provides additional information at no extra time or cost. As an additional benefit, phase images may be helpful to quantify iron accumulation, yet this is beyond the scope of our review.

Stability over Time

It is commonly believed that CMBs persist in the brain over many years (almost like the iron particles in a tattoo). A large population-based study in over 800 people, with more than 200 participants presenting with microbleeds, found that in only six people CMBs disappeared after 3.4 years of follow-up, whereas new CMBs developed in 85 other participants (20). A recent investigation, however, challenged this view and demonstrated decrease in both number and quantitative susceptibility (21). It remains to be determined whether this observation is true only for the investigated military service members with chronic traumatic brain injury, or whether these findings also apply to other CMBs (eg, in neurodegenerative disorders).

Visual Rating and Automatic Detection of CMBs

Visual rating scales have been shown to improve interrater reliability for both presence and anatomic location of CMBs. The two most commonly used validated scales are Microbleed Anatomic Rating Scale (MARS) (22) and Brain Observer MicroBleed Scale (BOMBS) (23), which both distinguish anatomic locations into lobar, deep, and infratentorial (including brainstem).

In addition to visual inspection, a number of automated tools have been proposed to detect CMBs, including in trauma (24), radiation encephalopathy (25), and multiple sclerosis (26). Especially when used at higher field strength, these methods might facilitate or improve visual rating (27), although many false-positives segmentations occur. Currently, these automated tools are in the stage of development and await clinical validation.

Quantitative Susceptibility Mapping

Quantitative susceptibility mapping (QSM) is a related MR imaging technique that aims to quantify relative tissue susceptibility, allowing to measure, for example, nonfocal iron deposition in neurodegenerative diseases (28,29). One interesting technical aspect of QSM is that susceptibility of a CMB is a physical property that is independent of echo time (30). Consequently, QSM might reduce the sequence dependence of CMB detection and thus facilitate standardization across studies and centers. Furthermore, QSM attempts to reconstruct the source of a local susceptibility perturbation, whereas SW imaging actually depicts the perturbing (dipole) field resulting from it. This dipole field causes the "blooming" effect on SW images, overestimating the CMB volume. Consequently, QSM should allow more accurate quantification of CMB volumes or burden. However, accurate quantification of CMB susceptibility is technically challenging (31) and the clinical relevance of QSM for detection of CMBs remains to be investigated.

Radiologic–Pathologic Correlation of CMBs

There are only a few published radiologic–histopathologic correlation studies of CMBs. One of the earliest studies assessed GRE T2*-weighted imaging in 11 brains of patients who died of

Figure 2

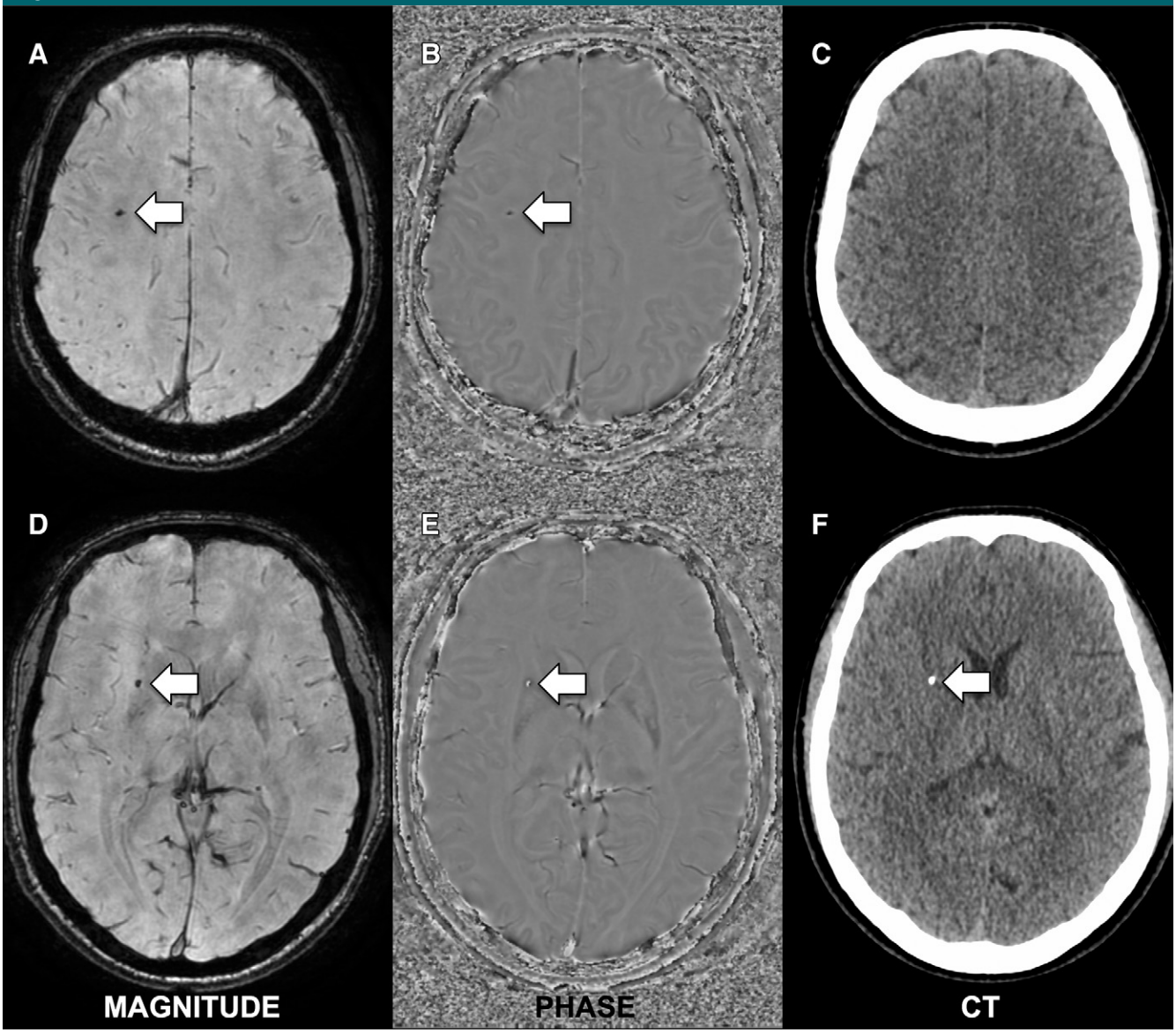

Figure 2: Images in a 49-year-old man undergoing imaging for assessment of headaches. *A, D,* Susceptibility three-dimensional multiecho T2*-weighted imaging at 3.0 T demonstrates two punctiform lesions compatible with cerebral microbleeds (CMBs) (arrows). *B, E,* Corresponding phase images show that lesion in right frontal white matter is predominantly hypointense and this lesion presumably corresponds to a CMB; second lesion in right external capsule and putamen is predominantly hyperintense. *C, F,* Corresponding CT images demonstrate no calcification and presence of microcalcification, respectively. As discussed in the Technical Considerations section, CMBs may appear hyperintense or hypointense in different MR systems depending on whether the imager uses a right- or left-handed coordinate system.

intracranial hemorrhage and found 34 areas of signal loss because of susceptibility (6). Histopathologic examination showed focal hemosiderin deposition in 21 of 34 areas of MR signal loss, corresponding to a true-positive rate of 62%. However, hemosiderin deposits were noted in two of 11 brains without corresponding MR imaging signal changes, relating to a false-negative rate of 18%. Another study assessed one brain of a woman with hypertension with nine CMB-like lesions depicted at premortem imaging. Eight lesions were confirmed on pathologic correlation (true-positive rate, 89%); one CMB observation was false-positive (false-positive rate, 11%) (32). A more recent study assessed SW imaging in 10 patients with CAA (33). Among 38 suspected CMBs at MR imaging, the true-positive rate at histopathologic analysis was 48% (16 of 38), whereas the false-positive rate was 24% (33). In a meta-analysis of 85 CMBs in

18 patients (34), 13 of the suspected CMBs were not associated with specific pathology at microscopy for an overall false-positive rate (areas of MR susceptibility because of other causes) of 19%. A more recent investigation that assessed 25 patients with 31 potential CMBs depicted by using premortem T2*-weighted imaging at 1.5 T and 3.0 T (35) found a true-positive rate of 52%, and a false-positive rate of 13%. The additionally performed postmortem MR imaging found additional CMBs only in a minority of patients and could therefore exclude the possibility that many CMBs occurred in the interval between premortem clinical MR imaging and death. Moreover, almost every second patient had additional CMBs at histopathologic analysis compared with premortem clinical MR imaging (with $0.7 \times 0.7 \times 0.7$ mm^3 voxels at 3.0 T), resulting in a false-negative rate of premortem MR imaging of 48%. This is still likely an underestimation of the true number of CMBs, because histopathologic analysis can only examine a select number of sections and not the entire brain.

The location of superficial or lobar versus deep, as well as supratentorial versus infratentorial, is important for the interpretation of CMBs, as well as for the clinical implications (discussed in the following sections). Both hypertensive small vessel disease and CAA contribute to the formation of lobar CMBs, whereas CMBs located in the basal ganglia or in infratentorial brain regions are mainly associated with hypertensive vasculopathy (Fig 3) (36,37).

In summary, for the currently used clinical protocols ranging from 1.5 T to 3.0 T, and from two-dimensional GRE T2*-weighted to SW imaging and a wide range of underlying pathologies (6,32,33,35,38), the true-positive rates for CMBs depicted at imaging are 48%–89%, the false-positive rates are 11%–24%, and the false-negative rates are 18%–48%. False-positive CMB findings include mimics such as microdissections, microaneurysms, microcalcifications, and arteriolar pseudocalcifications (6,32,33).

The correspondence between MR imaging and histopathologic analysis in CMBs is much better at 7.0 T for various diseases (39), likely because of the higher sensitivity of 7.0 T for small hemosiderin deposits. Although 7.0 T is unavailable for routine clinical use, it does show that with appropriate instrumentation, MR imaging has very good sensitivity for CMB detection.

Figure 3

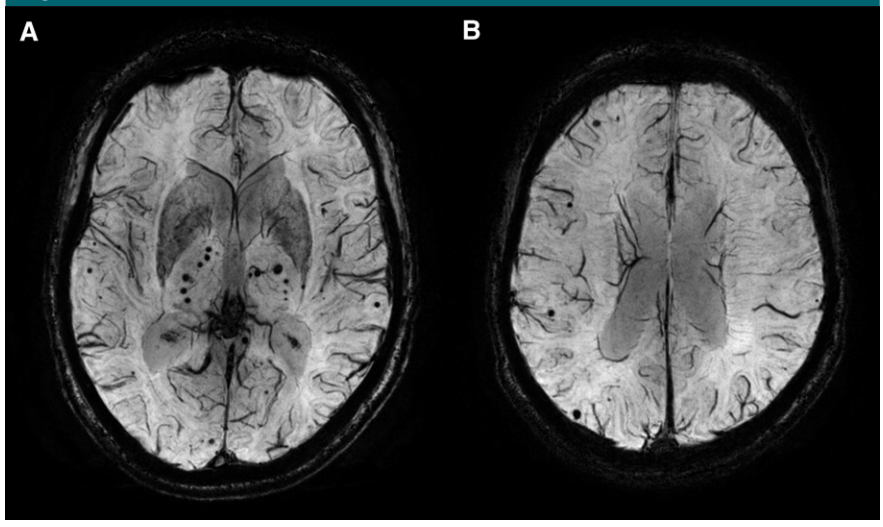

Figure 3: Susceptibility-weighted images show mixed pattern of, *A,* deep (thalamic) and, *B,* lobar (near the cortex) cerebral microbleeds, reflecting cerebrovascular risk factors and amyloid angiopathy, respectively.

Effect of the Presence of CMBs on Cognition

The cognitive repercussions of CMBs are a matter of debate (40–42). The two prevailing hypotheses are that CMBs either affect brain functioning through strategic disruptions of connections between brain regions (43–45), or that the underlying brain pathology—of which CMBs are reflective—causes (sub)clinical deficits (46,47).

Several studies reported associations of CMB location with performance on cognitive tasks both in cross-sectional and longitudinal studies, although with conflicting results. For example, in a prospective study of 518 consecutive adults without neurologic disorder, presence (odds ratio, 3.93; 95% confidence interval: 1.44, 10.74) and number (odds ratio, 1.26; 95% confidence interval: 1.01, 1.59) of CMBs were related to reduced Mini-Mental State Examination scores more than 1.5 standard deviation below the age-related average (48). Deep (basal ganglia, thalamus, and infratentorial) CMBs were associated with low performance in one study (49), whereas in the Rotterdam study, strictly lobar CMBs had the strongest impact on cognition (46). Another longitudinal study suggests that multiple CMBs or the presence of mixed microbleeds (both in deep and lobar locations) were associated with an increased risk for dementia (50), whereas others reported that lobar CMBs were associated with accelerated cognitive decline (51). In contrast, negative results have also been reported with no correlation being found between location of CMBs and cognitive symptoms in a study of 328 cognitively intact, community-dwelling control participants and 72 participants with mild cognitive impairment (52).

In addition, there is no clear correlation between the presence of CMBs on MR images and cognitive symptoms in healthy control participants (52). Over time, the number of CMBs increases in longitudinal studies of normal aging (20,53) and dementia (54).

Overall, the correlation between the location as well as number of CMBs and cognitive symptoms is somewhat inconsistent and not very strong. This might be

not surprising when taking into account that the detection of CMBs depends on MR sequence characteristics, and that a substantial number of CMBs are missed in current clinical (premortem) MR imaging, as discussed in the previous sections. Consequently, current clinical MR imaging probably picks up only the tip of the iceberg, and those lesions that are depicted consequently correspond poorly with cognitive symptoms.

Aging and Other Risk Factors for CMBs

CMBs are relatively common in aging patients without known neurologic disease, although with lower prevalence than in patients with CAA and AD. As noted previously, the actual detection rate of CMBs will depend strongly on technical factors, and also on the populations studied. Large-scale epidemiologic studies report that CMB prevalence in aging participants (age >45 years) ranges from 5% to 35% (52,55–58), partly reflecting variation in the mean age of the population and in MR imaging technique used, which is also summarized in a recent overview article (59). To mention a few of the larger population-based studies examining CMB prevalence: In the Age, Gene/Environment Susceptibility–Reykjavik Study of 1962 participants (mean age, 76 years), the incidence was 11.1% with a two-dimensional echo-planar imaging–based GRE sequence (57). The Framingham Heart Study with two-dimensional T2*-weighted GRE images (5-mm sections, 2-mm gap) estimated a prevalence of 8.8% in their population (mean age, 66.5 years) (55). In the Rotterdam study of 4759 participants (mean age, 63.8 years) with a three-dimensional T2*-weighted sequence, prevalence was 18.7% (58), increasing to over 35% in those aged over 80 years (56). Still, the above studies seem to underestimate the true CMB prevalence, because histopathologic studies found a prevalence of 60%–70% in individuals who are very old (60–62).

Risk Factors for CMBs

Population-based studies find strong associations with age, hypertension (especially for deep CMBs), and a slightly higher prevalence in men (56,63). Given the fact that carrying the APOE4 gene increases the risk of lobar CMBs and that parietal regions are most frequently affected (64–66), it is likely that these CMBs in asymptomatic individuals represent a form of CAA, possibly in the setting of incipient AD. This is especially true for lobar CMBs; deep CMBs are more related to classic cerebrovascular risk factors, particularly hypertension. CMBs are more frequent in patients with hypertensive encephalopathy (1) and are strongly correlated with burden of white matter hyperintensities (67,68).

CMBs in Dementia and CAA

CMBs in AD and CAA have overlapping risk factors and pathologic correlates, and both diseases show a clearly higher prevalence and incidence of CMBs compared with normal aging (3,69). CAA is a disease (either sporadic or familial) caused by abnormal amyloid deposition in the vessel wall leading to CMBs and intracerebral macroscopic hemorrhage. Amyloid angiopathy can also occur in the setting of AD (with deposition of amyloid in the parenchyma and vessel wall) leading to CMBs and superficial siderosis, but without macroscopic bleeding. Reflective of their shared pathophysiologic mechanisms, both AD and CAA can be accompanied by superficial siderosis, occurring almost invariably in the presence of lobar CMBs (70,71).

Even with sensitive imaging techniques, prevalence of CMBs in AD is well below 100%, hampering its use as a diagnostic marker, because their absence has low negative predictive value to exclude AD. Although patients with mild cognitive impairment who progress to AD tend to have slightly more CMBs, most patients with mild cognitive impairment will not display any CMBs at current clinical field strengths (40,41). On the other hand, many other causes of CMBs exist, also limiting the positive predictive value if CMBs are detected, although a lobar pattern is certainly supportive in the appropriate setting. As discussed previously, the detection rate of CMBs depends on magnetic field strength and MR sequence. Combining several studies, we can summarize the correlation between the number of CMBs and cognitive decline (16,40–42,49,72). Simply put, two or more CMBs at T2*-weighted imaging and three or more CMBs at SW imaging are more likely in patients with mild cognitive impairment or early dementia. Increasing CMB load might predict further cognitive decline. Although the average ratio of CMBs at baseline did not differ between control participants and mild cognitive impairment (11% and 14%, respectively) more than three CMBs were present only within the group with progressive mild cognitive impairment (40). Similarly, another study reported a higher occurrence of CMBs in patients with progressive mild cognitive impairment (eight of 26) compared with patients with stable mild cognitive impairment (one of 23) (41). Taking into account the variation in CMB detection based on the MR methodology, this might indicate that two or more CMBs at T2*-weighted imaging and three or more CMBs at SW imaging might suggest increased risk of cognitive decline, which remains to be confirmed in large-scale prospective and controlled studies.

Moreover, antiamyloid treatments for AD are more likely to induce both amyloid-related imaging abnormalities suggestive of vasogenic edema, sulcal effusions, microhemorrhages, and hemosiderin deposits as complication of treatment in the presence of CMBs. Therefore, in addition to diagnostic information, the presence of CMBs might indicate increased risk of complication during the antiamyloid treatments for AD, yet future research is needed to clarify this issue.

By contrast, in patients with definite (histopathologically proven) CAA, the prevalence of CMBs is 100%, which is not true for superficial siderosis. In fact, a diagnosis of probable CAA can be made based on imaging findings, including CMBs (73). The distribution of CMBs in CAA is typically lobar, reflecting the histopathologic finding of

Figure 4

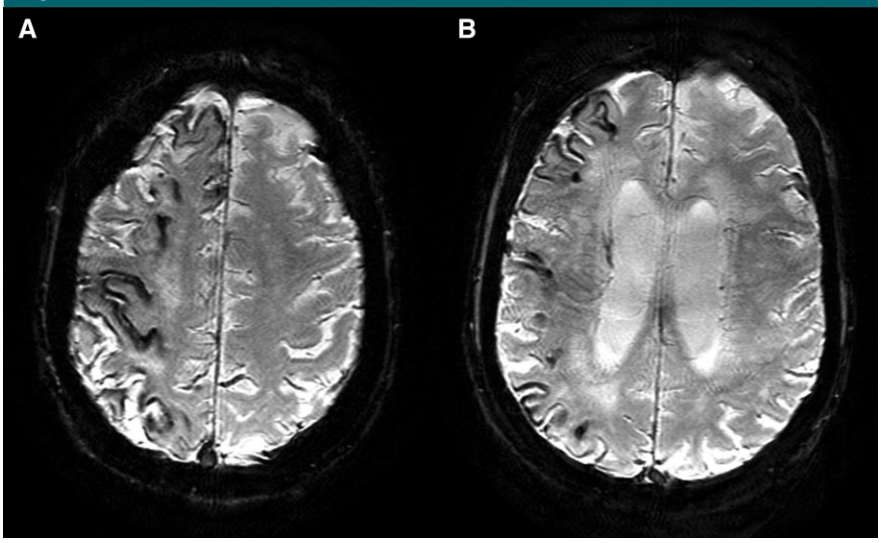

Figure 4: *A, B,* Axial susceptibility-weighted images show superficial siderosis (subpial linear deposits of susceptibility) at frontal-parietal convexity and probable cerebral microbleeds (CMBs) in a 83-year-old man with Alzheimer dementia (AD) without history of trauma or subarachnoid hemorrhage. Superfical siderosis tends to occur in conjunction with CMBs but may occur in isolation in AD.

amyloid angiopathy in cortical vessels. A similar lobar distribution pattern is observed in patients with AD. Involvement of leptomeningeal vessels probably underlies the occurrence of superficial siderosis that can be observed in both CAA and AD (71) (Fig 4). In one study of AD, having eight or more CMBs at 1.5 T was related to more severe disease parameters, including amyloid status and cognition (74), although the exact cutoff will be dependent on various technical factors as discussed previously.

An observation directly linking CMBs with amyloid angiopathy is the appearance of new CMBs during treatment with amyloid-lowering therapies, especially those targeting amyloid removal through immunization. The most likely explanation of these so-called amyloid-related imaging abnormalities is an altered pathway of amyloid metabolism involving the vessel wall, leading to increased fragility and occurrence of CMBs—as well as edema and sulcal effusions. Whatever the exact mechanism, the development of amyloid-related imaging abnormalities experimentally links CMBs to vascular amyloid in AD. Interestingly, amyloid-related imaging abnormalities may also occur spontaneously in patients with CAA—a phenomenon that can be treated with steroids (Fig 5).

CMBs occur more frequently in patients with vascular dementia (65% at T2*-weighted imaging, 86% at SW imaging) compared with patients with a prodromal status of AD—that is, mild cognitive impairment (20% at T2*-weighted imaging, 41% at SW imaging) or AD (18% at T2*-weighted imaging, 48% at SW imaging) (3,16). In patients with vascular cognitive impairment or frank vascular dementia, CMBs tend to be found in a central distribution pattern, affecting the thalamus, brainstem, and sometimes cerebellum, and are thus different from the lobar distribution in CAA and AD (63).

Traumatic Brain Injury

Moderate and severe traumatic brain injury is commonly associated with evident findings at CT or MR imaging, such as intracranial hemorrhage and cerebral contusions. The choice of imaging modality depends on local setting (eg, integration of CT into emergency department), availability, and condition of the patient (eg, easier to image an intubated patient by using CT), but CT is often the primary method. MR imaging is added later to depict diffuse axonal injury in patients with worse clinical conditions than can explained by the CT findings.

Imaging of mild traumatic brain injury is, in general, more challenging because trauma-related changes are subtler and consequently more difficult to detect. Typical imaging findings in mild traumatic head injury include nonhemorrhagic and hemorrhagic diffuse axonal injury (75). In hemorrhagic diffuse axonal injury, CMBs are typically located in the corpus callosum and at the gray-white matter junction, and in general have a more radial configuration following the perivascular spaces (Fig 6) compared with the more spherical CMBs occurring, for example, during neurodegeneration or hypertension (76). The prognostic implications of CMBs in mild traumatic head injury are being addressed only recently (77,78), and future work is needed.

CT versus MR Imaging

The sensitivity to depict nonhemorrhagic diffuse axonal injury is 0% at CT versus 11% at MR imaging, whereas the detection rate of hemorrhagic diffuse axonal injury is 22% at CT versus 47% at MR imaging (79). Moreover, MR imaging is more sensitive to depict subtle parenchymal traumatic lesions, and consequently is the modality of choice for mild traumatic brain injury.

Timing of Imaging

The CT density of the hemorrhage in CMBs rapidly decreases over days and they become isodense to brain after around 7–10 days. Consequently, the sensitivity of CT to depict CMBs is best during the first few days after mild traumatic brain injury.

On MR images, CMBs tend to remain visible long after mild traumatic brain injury. A recent article challenges this view and demonstrated regression of the number of CMBs over time in military service members with chronic

Figure 5

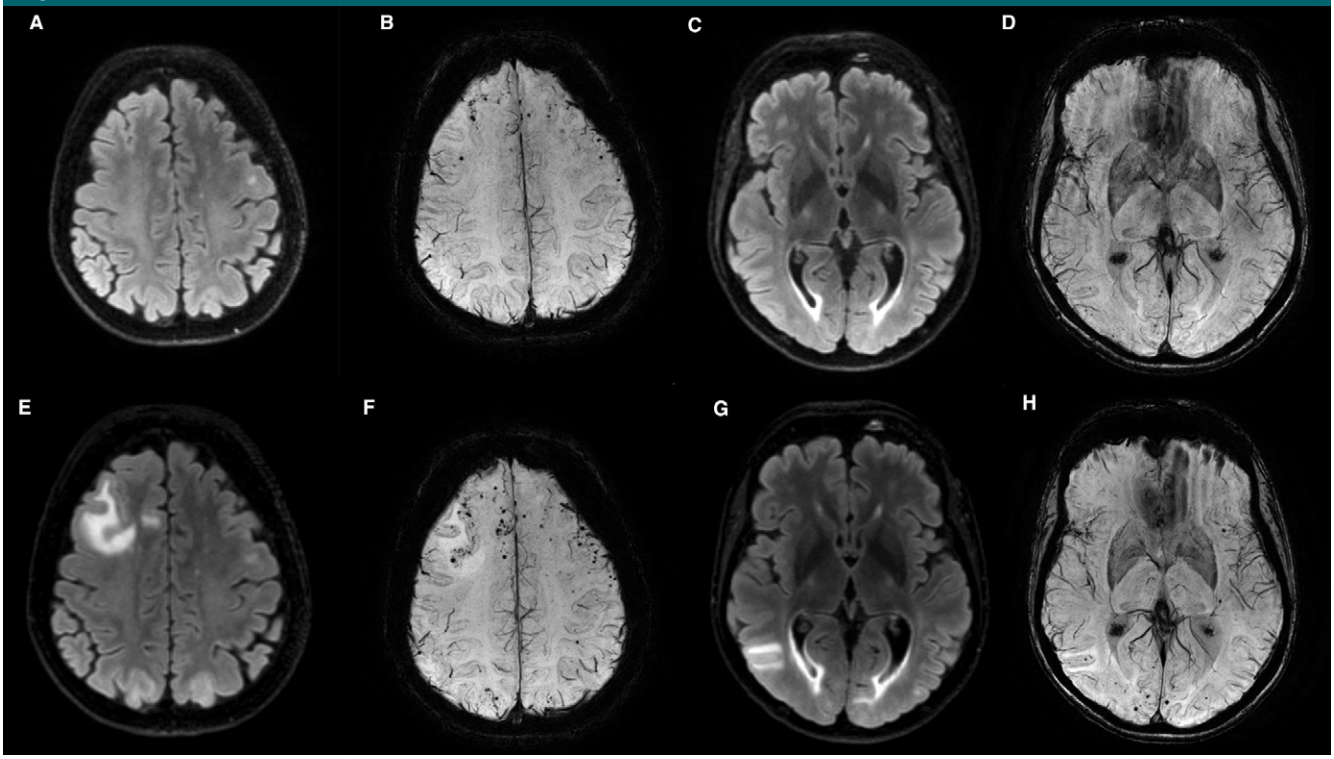

Figure 5: Images in a 64-year-old woman who was diagnosed with cerebral amyloid angiopathy almost 2 years ago based on fluctuating cognitive disturbances and aphasia. Baseline imaging (top row) demonstrates multiple lobar cerebral microbleeds (CMBs) on susceptibility-weighted images. Although clinically stable, follow-up MR imaging (bottom row) revealed new areas of hyperintensity and swelling in frontal and temporal lobes on fluid-attenuated inversion recovery images with an increase in number of CMBs. Previous occurrences and periods of clinical deterioration had been responsive to steroid treatment.

traumatic brain injury (21). This observation remains to be replicated in other domains and larger-scale studies, yet it indicates that MR imaging should ideally be performed early after mild traumatic brain injury, notably because the detection rate of nonhemorrhagic diffuse axonal injury features (eg, areas of diffusion restriction) is also higher in the immediate posttraumatic period. Moreover, intriguing recent reports indicate that CMBs may show dynamic changes after the acute injury, including growth (80) and temporary disappearance (81). These reports further support that the timing of imaging is important, but this needs confirmation in future studies.

Radiation-induced CMBs

Radiation-induced vascular injury can affect large vessels and, more commonly, small arteries and capillaries. Chronic radiation-induced endothelial damage leads to fibrinoid necrosis, vessel wall thickening, increased permeability, and thrombosis. CMBs as markers of radiation-induced small vessel disease are commonly seen following radiation therapy of pediatric brain tumors, but occur also in adults (Fig 7). A recent study including 190 patients (82) who had undergone radiation therapy for pediatric primary brain tumors found CMBs and cavernomas in over 40%. Another study of 149 survivors of pediatric brain tumors (83) found a cumulative incidence of CMB of 49%, with a rate that was four times higher after whole-brain irradiation compared with local therapy. CMB after radiation therapy correlates with worse executive function and temporal lobe CMB with a decrease in verbal memory. In adult patients undergoing radiation therapy for glioma or metastases, CMBs were found in 47% after a latency period ranging from 3 months to 9 years (mean, 33 months) (84). The frequency of CMBs was significantly associated with radiation dose and no CMBs were observed in regions that had received less than 25 Gy.

Serial imaging at 7.0 T in adult patients with cerebral gliomas of variable World Health Organization grade (85) showed that CMBs occurred only in those patients who had undergone radiation treatment. Microhemorrhages appeared approximately 2 years after radiation therapy, showing a higher prevalence with increasing time since completion of radiation therapy. A recent longitudinal study (86) suggested that patients treated with antiangiogenic agents had overall fewer CMBs and showed a significant reduction in the rate of new CMB formation, possibly indicating a radioprotective

Figure 6

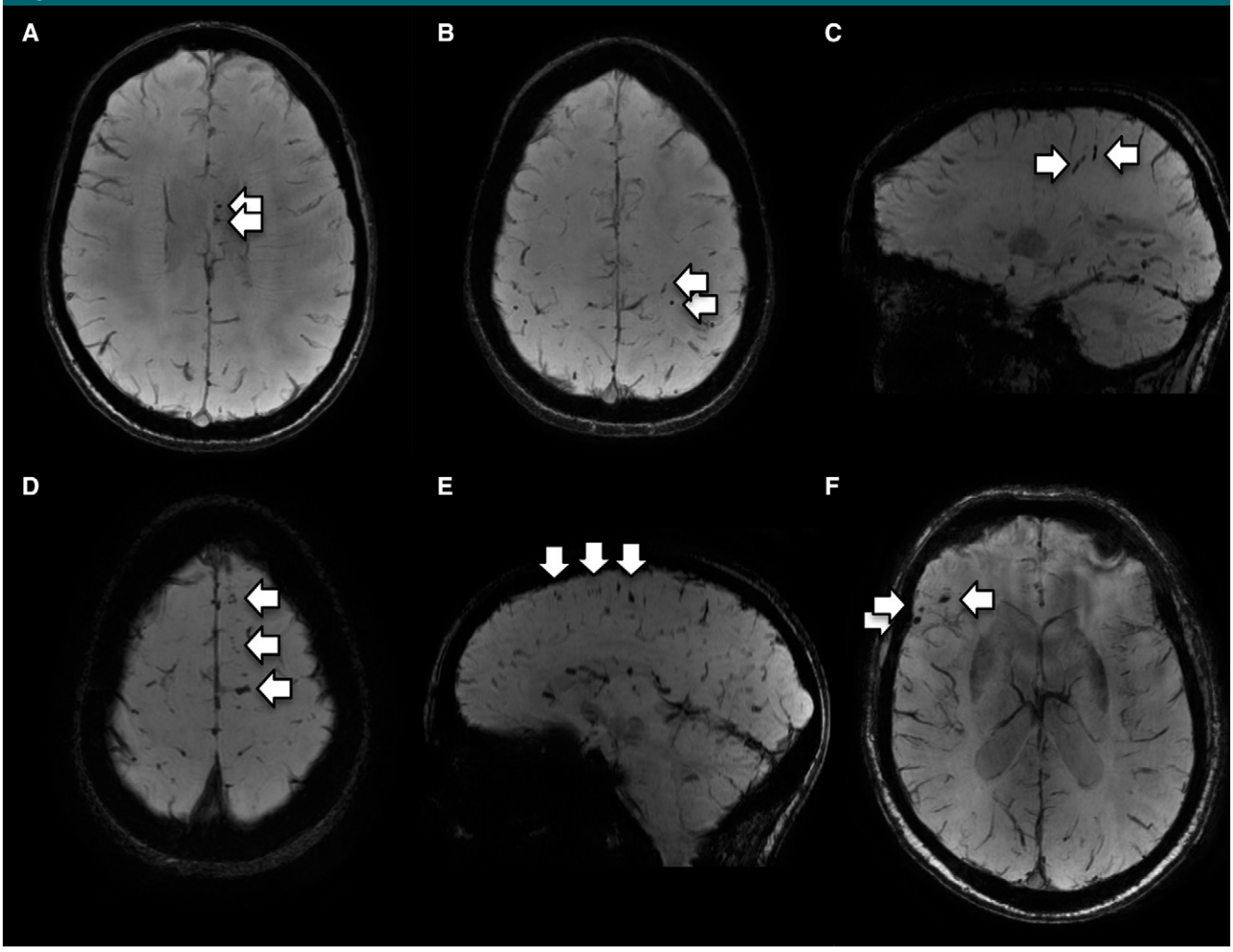

Figure 6: Images show collection of typical posttraumatic cerebral microbleeds (CMBs) (arrows), also referred to as hemorrhagic diffuse axonal injuries in this clinical context. *A–C,* Images in a 19-year-old woman after horseback riding accident. Location of diffuse axonal injury in, *A,* corpus callosum and, *B,* radial orientation in fronto-parietal white matter following perivascular spaces are typical, and better appreciated at, *C,* sagittal reconstruction. *D, E,* Images in a 39-year-old woman after mild traumatic head injury with multiple hemorrhagic diffuse axonal injuries, notably in left superior frontal gyrus. Typical radial orientation of lesions is again better appreciated at, *E,* sagittal reconstruction. *F,* Susceptibility-weighted angiography image in a 53-year-old man with mild to moderate traumatic brain injury 7 years prior to imaging. Hemorrhagic diffuse axonal injuries are present in left inferior frontal gyrus, illustrating that CMBs may be visualized years after traumatic brain injury.

effect of antiangiogenic drugs on the microvasculature.

In summary, CMBs appear to occur in at least 50% of patients who have undergone radiation treatment, in pediatric as well as in adult patients. The rate of CMB formation increases significantly 2 years after radiation treatment and an independent association between radiation-induced CMB and cognitive performance has been demonstrated.

CMBs in Other Diseases

Cavernous Angioma

Although cavernous angiomas (also called cavernous malformations) are generally well characterized at imaging because of their distinct appearance on T1-weighted (popcornlike spontaneous high signal intensity) and T2-weighted (hypointense hemosiderin ring) images, small so-called type IV (micro-) cavernous angiomas may be indistinguishable from CMBs at imaging (Fig 8) (87). Hemorrhage in cavernous angiomas can be classified into four types: type I, extralesional gross hemorrhage beyond cavernous angioma; type II, mixture of subacute and chronic hemorrhage; type III, area of hemosiderin with small central core; and type IV, area of hemosiderin deposition without central core (88). Thus, because of lack of the central core, the type IV lesions are only visible on SW images as

Figure 7

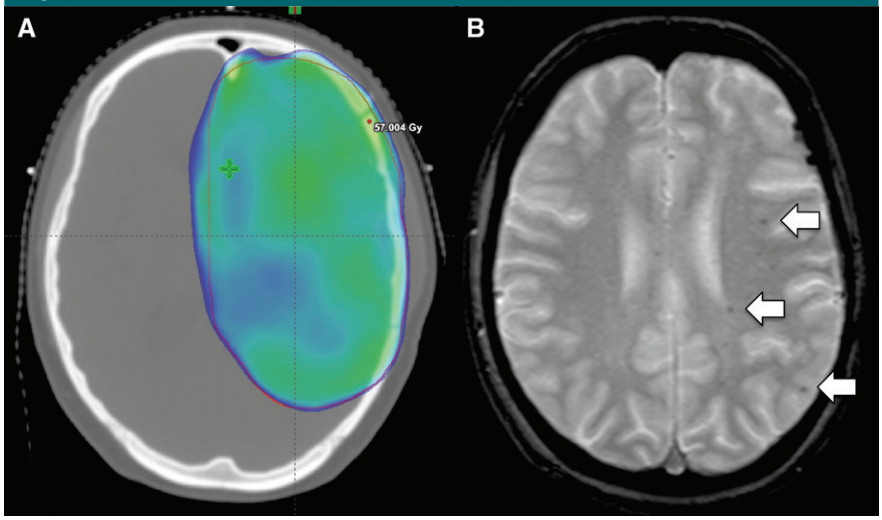

Figure 7: Images in a 32-year-old woman who underwent radiation therapy for World Health Organization grade IV glioma 5 years ago. *A,* CT image for radiation therapy planning shows radiation field (57 Gy line) overlying left frontal and parietal lobes. *B,* Axial T2*-weighted image demonstrates multiple cerebral microbleeds (CMBs) in left but not in right cerebral hemisphere (arrows). These CMBs lie within radiation field and were not present at MR imaging before radiation therapy.

hypointense dots, much like CMBs, and have been described as a distinct imaging type of cavernous angiomas in patients with familial cerebral cavernous malformations (89). Although only histologic examination can separate the two entities, for practical use, in patients without a family history and without evidence of classic cavernous angiomas at imaging, a hypointense lesion at SW imaging will most likely be a CMB.

Critical Medical Conditions

A number of critical medical conditions are associated with occurrence of CMBs and should be considered as causal factors when CMBs are encountered in critically ill patients without previous neurologic conditions (Fig 9). These conditions include infective endocarditis (90) (with microbleeds in over 50% of patients) (91), extracorporeal membrane oxygenation (92), and sepsis (93). Although the exact mechanism through which microbleeds develop in these conditions is unknown, hypotheses range from pyogenic vasculitis or subacute microvascular inflammatory processes (94) to endothelial dysfunction and microemboli (93). The location of microbleeds in endocarditis is predominantly cortical and it has been hypothesized that microbleeds represent a marker of disease severity (91). The clinical significance of microbleeds in these patients is currently a subject of debate. A prospective study of 130 patients with endocarditis by using MR imaging within 7 days of admission and before any surgical intervention found ischemic lesions in 68 patients and microhemorrhages in 74 patients, which lead to a modification in diagnosis and therapeutic plan in 24 patients (90).

Micrometastasis

Tiny metastases of primary tumors that tend to produce hemorrhagic brain metastases, such as melanoma, choriocarcinoma, lung cancer, and thyroid cancer, may sometimes resemble microbleeds. Note that the influence of melanin on T2* relaxation is minimal and the low signal in melanoma metastases appears to be caused by the presence of iron (95). Some of these may only be depicted on T2*-weighted or SW images and may not show any enhancement (Fig 10). A study comparing cerebral metastases of melanoma of lung cancer (96) found that melanoma metastases were five times more likely to demonstrate signal loss on T2*-weighted images than were lung metastases (42% vs 8%) and that eight of 120 melanoma metastases were only depicted on T2*-weighted images.

Cerebral Autosomal Dominant Arteriopathy with Subcortical Infarcts and Leukoencephalopathy

Cerebral autosomal dominant arteriopathy with subcortical infarcts and leukoencephalopathy is an inherited disorder because of a mutation in the *NOTCH3* gene on chromosome 19q12. Clinical presentations include progressive cognitive decline, migraine with aura, mood disturbances, and small vessel infarcts. CMBs have been found in 31%–69% of patients with this disease and are most commonly located in the thalamus, basal ganglia, and brainstem (Fig 11) (97). Other hallmarks of the disease are confluent white matter hyperintensities extending into the external capsules and temporal poles.

Fabry Disease

Fabry disease is an X-linked lysosomal storage disorder resulting in vascular glycosphingolipid accumulation and increased risk of stroke. MR imaging findings include white matter hyperintensities and CMBs. The prevalence of microbleeds in Fabry disease ranges between 15% and 30% (our own cohort of 34 patients with a median age of 44 years [98,99]) and appears to be higher in male patients and in patients with renal involvement.

Moyamoya Disease

Moyamoya disease is an idiopathic, progressive, nonarteriosclerotic, stenoocclusive disease of the distal internal carotid arteries and their proximal branches, resulting in the development of an extensive collateral vessel network at the base of the brain. Approximately 10% are related to specific gene mutations. There is an increased incidence of microbleeds in patients with moyamoya disease, which appears to be higher in patients of Asian descent (around 30%) compared with Europeans affected by

Figure 8

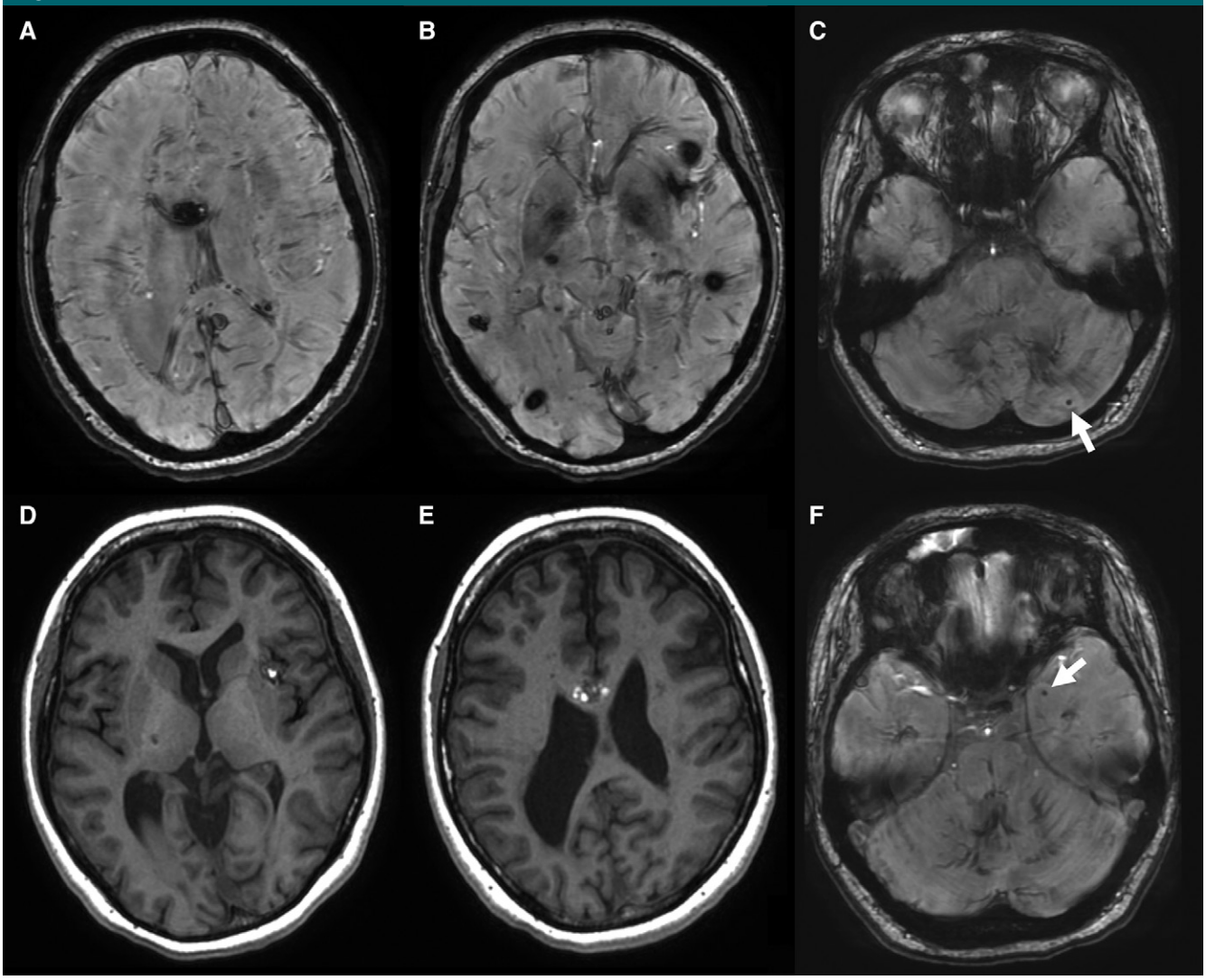

Figure 8: *A, B, C, F,* Axial susceptibility-weighted and, *D, E,* axial T1-weighted images in a 33-year-old patient with familial cavernous angiomas show microbleed-like hypointense dots in left cerebellum and left temporal lobe (arrows), as seen in supertentorial images. Small hypointense lesions (arrows in *C* and *F*) most likely represent type IV cavernomas.

this condition (13%) (100). CMBs in moyamoya disease are predictors of future intracerebral hemorrhage, which is more frequently an initial symptomatic event in patients of Asian descent.

Cardiac Valve Replacement

In a prospective study in patients with cardiac valve surgery, 12 of 19 patients developed a total of 26 small postoperative CMBs, indicating that the development of CMBs might be a common finding in this clinical setting (101).

CMBs and Stroke with Implications for Antithrombotic Treatment and Thrombolysis

CMBs are associated with an increased risk of both ischemic and hemorrhagic stroke. The population-based Rotterdam study (58) showed that participants with microbleeds in a lobar distribution (suggestive of CAA) had a higher risk of intracranial hemorrhage, whereas microbleeds in other locations were associated with increased risk of both ischemic and hemorrhagic stroke. A recent meta-analysis (102) of over 5000 patients with a mean follow-up period of 18 months demonstrated that a higher microbleed burden was related to an increased risk of ischemic stroke and intracerebral hemorrhage, with the risk of the latter increasing much more steeply. In patients with more than five microbleeds, the relative risk of intracerebral hemorrhage was 14.1 compared with 2.7 for ischemic stroke. For patients presenting initially with intracerebral

Figure 9

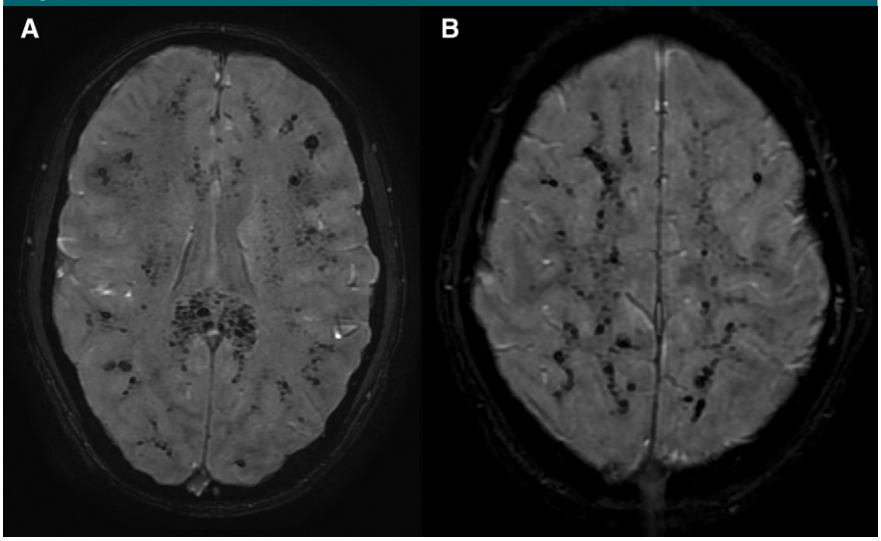

Figure 9: *A, B,* Images in a 16-year old boy admitted to intensive care unit with sepsis. There are widespread microbleeds in the cortico-subcortical regions, as well as the corpus callosum.

Figure 10

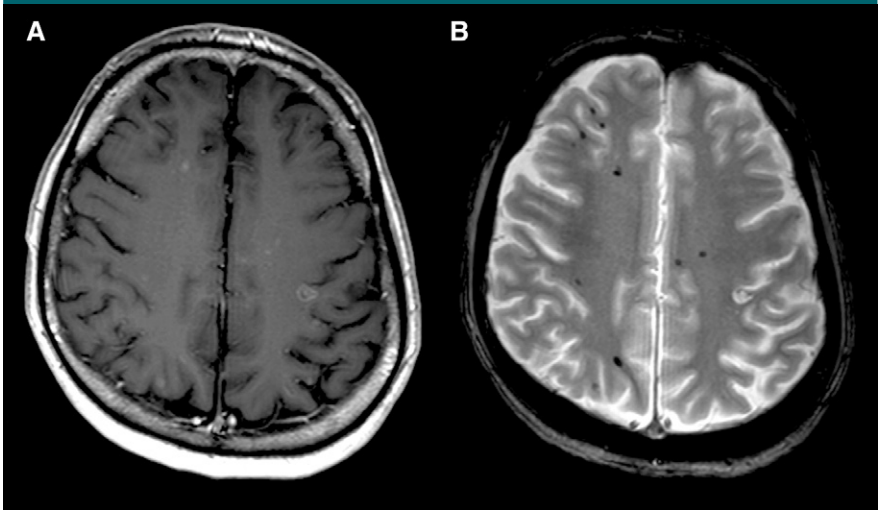

Figure 10: Images in a 74-year-old man with cerebral metastases from small cell carcinoma of the lung. *A,* Axial contrast-enhanced T1-weighted image demonstrates several small enhancing nodules in both cerebral hemispheres, mostly near gray-white matter junction. *B,* Axial T2*-weighted image demonstrates that many of these lesions show susceptibility artifact. Some tiny additional lesions in right frontal lobe are not readily visible on contrast-enhanced images.

hemorrhage, the annual risk of repeat hemorrhage depends on the location of the initial intracerebral hemorrhage. This risk is higher for lobar hemorrhages (103), more likely to be caused by CAA. MR imaging plays an increasing role in the diagnostic work-up of intracerebral hemorrhage and can help confirm the presence of peripheral CMBs suggestive of CAA as underlying cause (Fig 12). MR imaging can furthermore reveal cortical superficial siderosis (Fig 13), another imaging marker for CAA that increases the risk of future intracerebral hemorrhage (104).

This increase of intracerebral hemorrhage in the presence of CMBs has led to concerns regarding the safety of antithrombotic drugs in secondary stroke prevention, as well as thrombolysis in acute stroke. The debate in this field is currently impeded by the lack of large, prospective studies of CMBs in stroke cohorts, but several studies are presently underway (Clinical Relevance of Microbleeds in Stroke study [CROMIS-2] and Intracerebral Hemorrhage in Patients Taking Oral Anticoagulant for Atrial Fibrillation With Cerebral Microbleeds [IPAAC]) (105). Recent meta-analyses in patients with ischemic stroke or transient ischemic attack who use antiplatelet agents suggest that the presence of CMBs may significantly increase the subsequent risk of intracerebral hemorrhage (106). A systematic review on use of warfarin and risk of intracerebral hemorrhage in the presence of microbleeds suggests that microbleeds increase the risk of warfarin-associated intracerebral hemorrhage (107).

From a clinical perspective, it is crucial to assess whether the CMB-related risk of intracerebral hemorrhage, if any, outweighs the benefits expected from antithrombotic therapy. This is a critical dilemma in patients who undergo anticoagulation therapy for atrial fibrillation and then developed intracerebral hemorrhage. Anticoagulants (non-vitamin K antagonists) or atrial appendage occlusion may represent an alternative treatment option in these patients. Large studies assessing the risk-benefit ratio of antithrombotic therapy are currently unavailable, but the existing evidence suggests that in patients with many microbleeds, lobar microbleeds, or other imaging markers of CAA such as cortical superficial siderosis, the risks may outweigh the benefits (108).

Finally, a recent comprehensive meta-analysis shows that CMBs are associated with greater risk of symptomatic intracerebral hemorrhage and

Figure 11

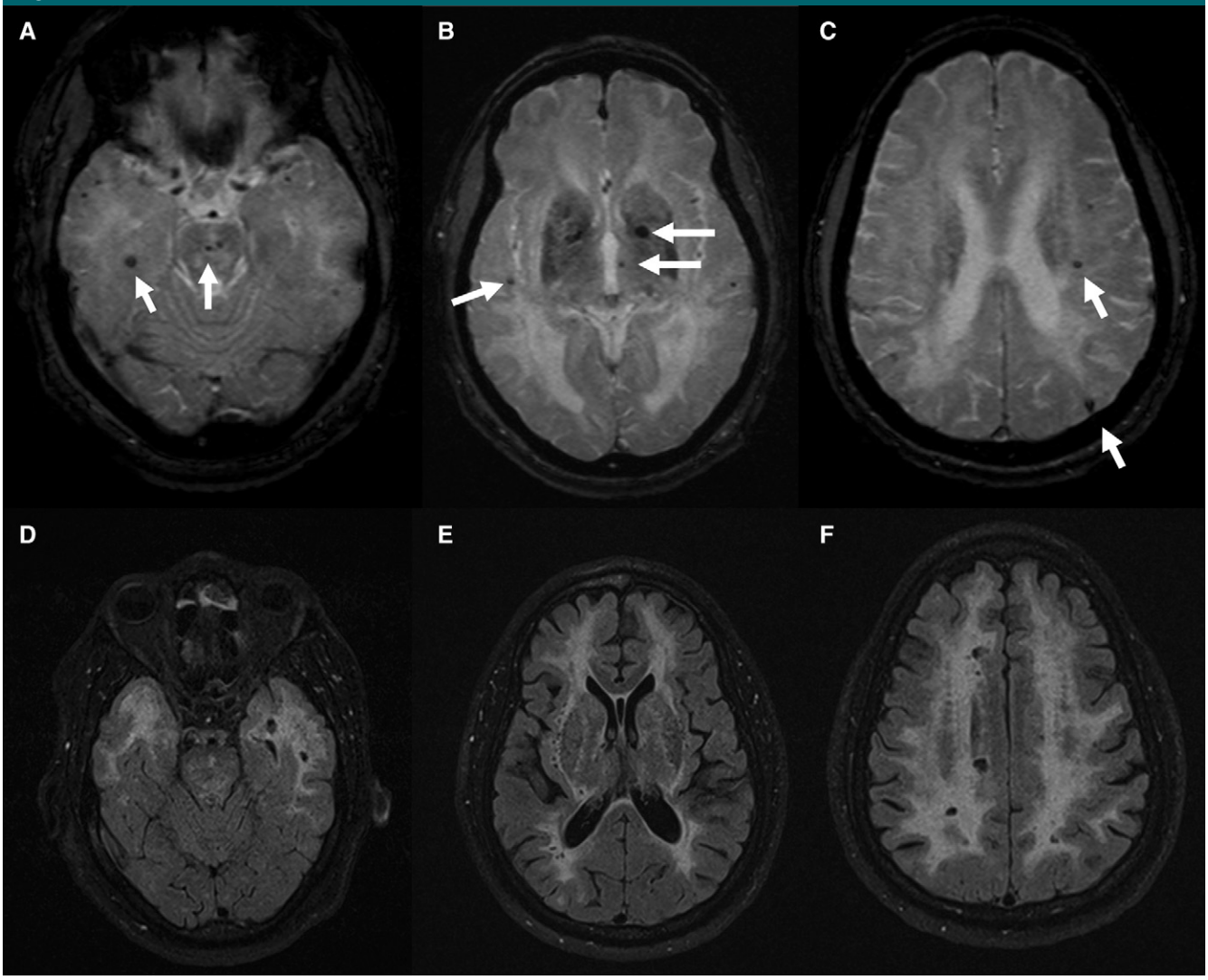

Figure 11: Images in a 52-year-old man with cerebral autosomal dominant arteriopathy with subcortical infarcts and leukoencephalopathy. *A–C,* Axial T2*-weighted images show multiple cerebral microbleeds in basal ganglia, thalamus, pons, and peripherally (arrows). *D–F,* Axial fluid-attenuated inversion recovery images demonstrate widespread, confluent white matter hyperintensities with involvement of external capsules and temporal poles, which is a typical feature of this disease.

poor functional outcome (34). How this knowledge can impact clinical practice remains uncertain because the vast majority of the stroke centers use CT and CT angiography for patient triage, particularly in the era of intravascular intervention.

In summary, there are currently no firmly established guidelines that anticoagulants, antiaggregation, or thrombolysis should be avoided in the presence of CMBs. This is likely to change in the near future, because data from ongoing prospective studies will become available. Future recommendations may take into account not only the presence but also the number and location of CMBs.

Conclusions

CMBs have attracted growing interest over the last years because of increased availability of high-field-strength MR systems and the development of dedicated imaging sequences leading to higher detection rate of CMBs in various diseases, as well as in asymptomatic patients. The imaging techniques currently used (1.5 T and 3.0 T, two-dimensional GRE T2*-weighted imaging, and SW imaging) significantly underestimate the true number of CMBs, with an estimated number of false-negative findings in the range of 50% when compared with histopathologic analysis as ground truth. The true-positive rate ranges from 48%–89%, and false-positive mimics of CMBs include

Figure 12

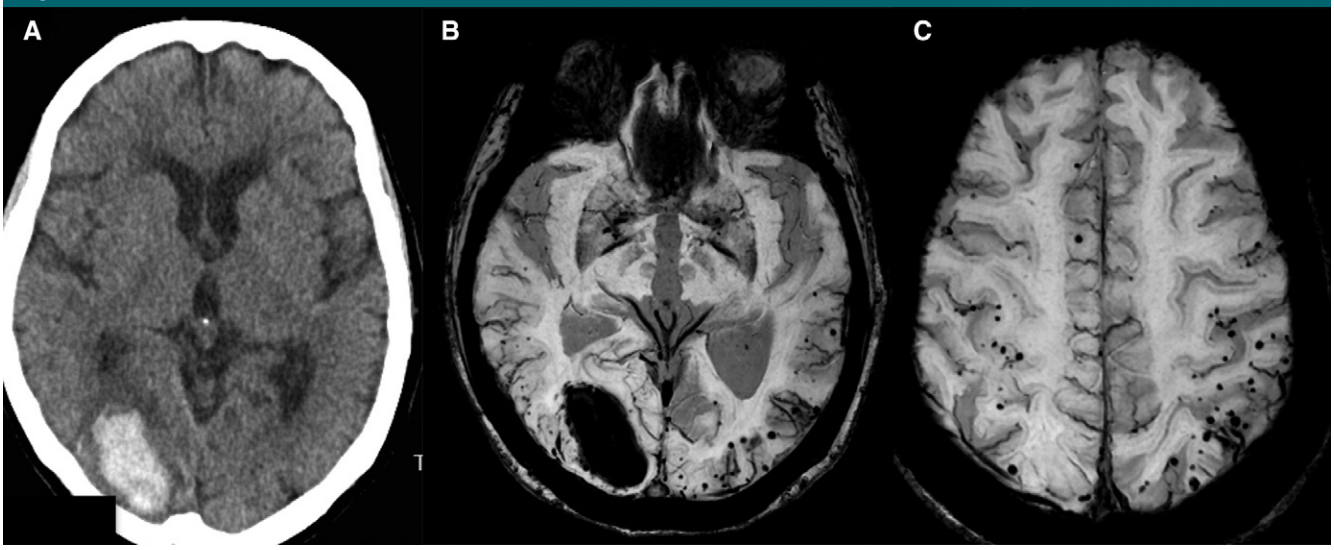

Figure 12: Images show hemorrhagic stroke in cerebral amyloid angiopathy (CAA). *A,* CT in a 79-year-old woman with right occipital hemorrhage demonstrates acute hyperdense hematoma. *B, C,* Susceptibility-weighted images reveal, in addition to acute hemorrhage, numerous peripheral lobar cerebral microbleeds in a distribution that is typical for CAA.

Figure 13

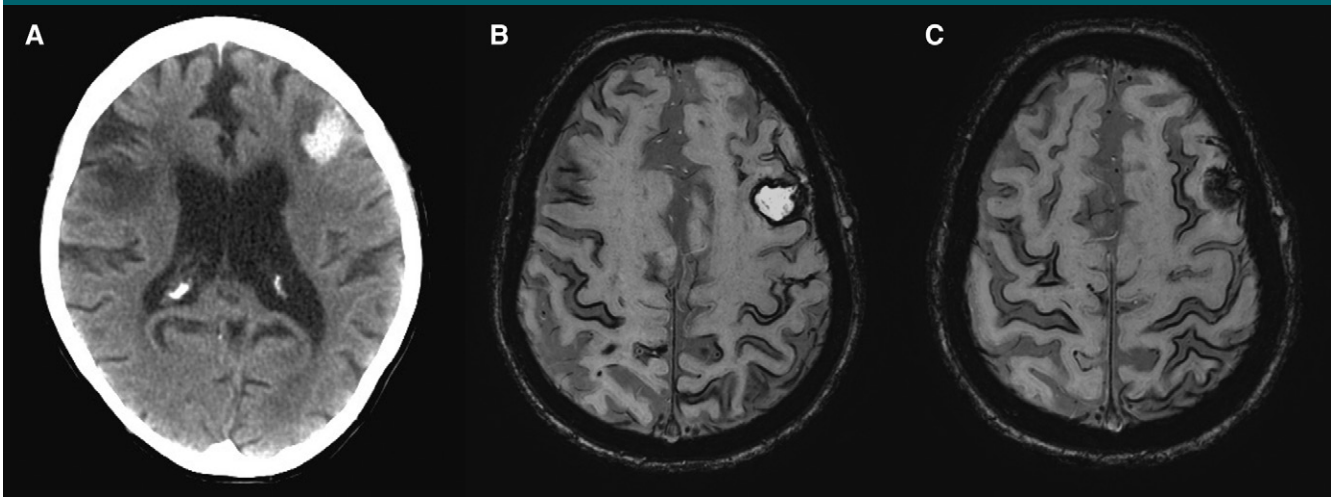

Figure 13: Images in an 81-year-old man with left frontal hemorrhage. *A,* CT image shows acute left frontal hematoma. *B, C,* Susceptibility-weighted (SW) images were acquired 10 days later. *C,* Center of subacute hematoma appears hyperintense on magnitude images of SW imaging sequence. In addition, there is diffuse cortical superficial siderosis causing susceptibility artifact over superior convexity sulci, another typical feature of cerebral amyloid angiopathy.

microdissections, microaneurysms, and microcalcifications. Phase images might be useful to differentiate microbleeds from calcifications. The fact that current clinical MR techniques only help to detect a part of the true number of CMBs might explain the varying and partially conflicting results regarding the clinical repercussions of CMBs and implies the need for further technical developments.

Despite this current imprecise imaging of CMBs, these lesions play an increasing role in the diagnosis of specific diseases such as CAA and cavernomatosis. Moreover, their contributions as risk factors for cognitive decline are increasingly recognized. The overlap between AD, vascular risk factors, and CAA might explain the increased prevalence of CMBs in these conditions, and explain the difficulty in disentangling the exact etiology of CMBs in some patients, despite the fact that the classic distribution of CMBs varies between these conditions.

In mild traumatic brain injury, hemorrhagic diffuse axonal injury is one of the most sensitive and long-lasting imaging markers. The configuration of these hemorrhagic diffuse axonal injuries is typically more linear and in a radial distribution compared with the typical CMBs discussed previously.

Finally, presence of multiple CMBs might increase the risk of hemorrhage during anticoagulation or antiaggregation and thrombolysis, and large-scale studies and subsequent guidelines are in development.

Disclosures of Conflicts of Interest: S.H. disclosed no relevant relationships. **M.W.V.** disclosed no relevant relationships. **J.P.A.K.** Activities related to the present article: disclosed no relevant relationships. Activities not related to the present article: institution received speakers' fees from Toshiba Medical Systems Europe. Other relationships: disclosed no relevant relationships. **E.M.L.** disclosed no relevant relationships. **H.R.J.** disclosed no relevant relationships. **F.B.** Activities related to the present article: disclosed no relevant relationships. Activities not related to the present article: is a consultant to Bayer-Schering, Biogen-IDEC, Genzyme, Janssen Research, Merck-Serono, Novartis, Roche, Synthon BV, and Teva; is a board member of *Brain*, *European Radiology*, *Neurology*, *Multiple Sclerosis Journal*, and *Radiology*; received grant from Dutch MS Society, EU-FP7/H2020; institution received payment from Biogen-IDEC and IXICO for development of educational presentations including service on speakers' bureaus. Other relationships: disclosed no relevant relationships.

References

1. Greenberg SM, Vernooij MW, Cordonnier C, et al. Cerebral microbleeds: a guide to detection and interpretation. Lancet Neurol 2009;8(2):165–174.
2. Goos JD, van der Flier WM, Knol DL, et al. Clinical relevance of improved microbleed detection by susceptibility-weighted magnetic resonance imaging. Stroke 2011;42(7):1894–1900.
3. Cordonnier C, van der Flier WM, Sluimer JD, Leys D, Barkhof F, Scheltens P. Prevalence and severity of microbleeds in a memory clinic setting. Neurology 2006;66(9):1356–1360.
4. Cordonnier C, Al-Shahi Salman R, Wardlaw J. Spontaneous brain microbleeds: systematic review, subgroup analyses and standards for study design and reporting. Brain 2007;130(Pt 8):1988–2003.
5. Greenberg SM, Nandigam RN, Delgado P, et al. Microbleeds versus macrobleeds: evidence for distinct entities. Stroke 2009;40(7):2382–2386.
6. Fazekas F, Kleinert R, Roob G, et al. Histopathologic analysis of foci of signal loss on gradient-echo T2*-weighted MR images in patients with spontaneous intracerebral hemorrhage: evidence of microangiopathy-related microbleeds. AJNR Am J Neuroradiol 1999;20(4):637–642.
7. Nandigam RN, Viswanathan A, Delgado P, et al. MR imaging detection of cerebral microbleeds: effect of susceptibility-weighted imaging, section thickness, and field strength. AJNR Am J Neuroradiol 2009;30(2):338–343.
8. Stehling C, Wersching H, Kloska SP, et al. Detection of asymptomatic cerebral microbleeds: a comparative study at 1.5 and 3.0 T. Acad Radiol 2008;15(7):895–900.
9. Bian W, Hess CP, Chang SM, Nelson SJ, Lupo JM. Susceptibility-weighted MR imaging of radiation therapy-induced cerebral microbleeds in patients with glioma: a comparison between 3T and 7T. Neuroradiology 2014;56(2):91–96.
10. Theysohn JM, Kraff O, Maderwald S, et al. 7 tesla MRI of microbleeds and white matter lesions as seen in vascular dementia. J Magn Reson Imaging 2011;33(4):782–791.
11. Conijn MM, Geerlings MI, Biessels GJ, et al. Cerebral microbleeds on MR imaging: comparison between 1.5 and 7T. AJNR Am J Neuroradiol 2011;32(6):1043–1049.
12. Brundel M, Heringa SM, de Bresser J, et al. High prevalence of cerebral microbleeds at 7Tesla MRI in patients with early Alzheimer's disease. J Alzheimers Dis 2012;31(2):259–263.
13. Haacke EM, Xu Y, Cheng YC, Reichenbach JR. Susceptibility weighted imaging (SWI). Magn Reson Med 2004;52(3):612–618.
14. Mittal S, Wu Z, Neelavalli J, Haacke EM. Susceptibility-weighted imaging: technical aspects and clinical applications, part 2. AJNR Am J Neuroradiol 2009;30(2):232–252.
15. Shams S, Martola J, Cavallin L, et al. SWI or T2*: which MRI sequence to use in the detection of cerebral microbleeds—the Karolinska Imaging Dementia study. AJNR Am J Neuroradiol 2015;36(6):1089–1095.
16. Uetani H, Hirai T, Hashimoto M, et al. Prevalence and topography of small hypointense foci suggesting microbleeds on 3T susceptibility-weighted imaging in various types of dementia. AJNR Am J Neuroradiol 2013;34(5):984–989.
17. Soman S, Holdsworth SJ, Barnes PD, et al. Improved T2* imaging without increase in scan time: SWI processing of 2D gradient echo. AJNR Am J Neuroradiol 2013;34(11):2092–2097.
18. Kaaouana T, de Rochefort L, Samaille T, et al. 2D harmonic filtering of MR phase images in multicenter clinical setting: toward a magnetic signature of cerebral microbleeds. Neuroimage 2015;104:287–300.
19. Li CQ, Imbesi SG, Lee RR, et al. Potential pitfalls when differentiating hemorrhage and calcium on susceptibility-weighted images. Neurographics 2016;6(3):123–126.
20. Poels MM, Ikram MA, van der Lugt A, et al. Incidence of cerebral microbleeds in the general population: the Rotterdam scan study. Stroke 2011;42(3):656–661.
21. Liu W, Soderlund K, Senseney JS, et al. Imaging cerebral microhemorrhages in military service members with chronic traumatic brain injury. Radiology 2016;278(2):536–545.
22. Gregoire SM, Chaudhary UJ, Brown MM, et al. The Microbleed Anatomical Rating Scale (MARS): reliability of a tool to map brain microbleeds. Neurology 2009;73(21):1759–1766.
23. Cordonnier C, Potter GM, Jackson CA, et al. Improving interrater agreement about brain microbleeds: development of the Brain Observer MicroBleed Scale (BOMBS). Stroke 2009;40(1):94–99.
24. van den Heuvel TL, van der Eerden AW, Manniesing R, et al. Automated detection of cerebral microbleeds in patients with traumatic brain injury. Neuroimage Clin 2016;12:241–251.
25. Bian W, Hess CP, Chang SM, Nelson SJ, Lupo JM. Computer-aided detection of radiation-induced cerebral microbleeds on susceptibility-weighted MR images. Neuroimage Clin 2013;2:282–290.
26. Zivadinov R, Ramasamy DP, Benedict RR, et al. Cerebral microbleeds in multiple sclerosis evaluated on susceptibility-weighted images and quantitative susceptibility maps: a case-control study. Radiology 2016;281(3):884–895.
27. Kuijf HJ, Brundel M, de Bresser J, et al. Semi-automated detection of cerebral microbleeds on 3.0 T MR Images. PLoS One 2013;8(6):e66610.
28. Langkammer C, Schweser F, Krebs N, et al. Quantitative susceptibility mapping (QSM) as a means to measure brain iron: a post mortem validation study. Neuroimage 2012;62(3):1593–1599.
29. Reichenbach JR, Schweser F, Serres B, Deistung A. Quantitative susceptibility mapping: concepts and applications. Clin Neuroradiol 2015;25(Suppl 2):225–230.

30. Liu T, Surapaneni K, Lou M, Cheng L, Spincemaille P, Wang Y. Cerebral microbleeds: burden assessment by using quantitative susceptibility mapping. Radiology 2012;262(1):269–278.

31. Cronin MJ, Wang N, Decker KS, Wei H, Zhu WZ, Liu C. Exploring the origins of echo-time-dependent quantitative susceptibility mapping (QSM) measurements in healthy tissue and cerebral microbleeds. Neuroimage 2017;149:98–113.

32. Tatsumi S, Shinohara M, Yamamoto T. Direct comparison of histology of microbleeds with postmortem MR images: a case report. Cerebrovasc Dis 2008;26(2):142–146.

33. Schrag M, McAuley G, Pomakian J, et al. Correlation of hypointensities in susceptibility-weighted images to tissue histology in dementia patients with cerebral amyloid angiopathy: a postmortem MRI study. Acta Neuropathol (Berl) 2010;119(3):291–302.

34. Charidimou A, Shoamanesh A; International META-MICROBLEEDS Initiative. Clinical relevance of microbleeds in acute stroke thrombolysis: comprehensive meta-analysis. Neurology 2016;87(15):1534–1541.

35. Haller S, Montandon ML, Lazeyras F, et al. Radiologic-histopathologic correlation of cerebral microbleeds using pre-mortem and post-mortem MRI. PLoS One 2016;11(12):e0167743.

36. Park JH, Seo SW, Kim C, et al. Pathogenesis of cerebral microbleeds: in vivo imaging of amyloid and subcortical ischemic small vessel disease in 226 individuals with cognitive impairment. Ann Neurol 2013;73(5):584–593.

37. Yakushiji Y, Yokota C, Yamada N, Kuroda Y, Minematsu K. Clinical characteristics by topographical distribution of brain microbleeds, with a particular emphasis on diffuse microbleeds. J Stroke Cerebrovasc Dis 2011;20(3):214–221.

38. Shoamanesh A, Kwok CS, Benavente O. Cerebral microbleeds: histopathological correlation of neuroimaging. Cerebrovasc Dis 2011;32(6):528–534.

39. De Reuck J, Deramecourt V, Auger F, et al. Post-mortem 7.0-tesla magnetic resonance study of cortical microinfarcts in neurodegenerative diseases and vascular dementia with neuropathological correlates. J Neurol Sci 2014;346(1-2):85–89.

40. Ayaz M, Boikov AS, Haacke EM, Kido DK, Kirsch WM. Imaging cerebral microbleeds using susceptibility weighted imaging: one step toward detecting vascular dementia. J Magn Reson Imaging 2010;31(1):142–148.

41. Kirsch W, McAuley G, Holshouser B, et al. Serial susceptibility weighted MRI measures brain iron and microbleeds in dementia. J Alzheimers Dis 2009;17(3):599–609.

42. Haller S, Bartsch A, Nguyen D, et al. Cerebral microhemorrhage and iron deposition in mild cognitive impairment: susceptibility-weighted MR imaging assessment. Radiology 2010;257(3):764–773.

43. Heringa SM, Reijmer YD, Leemans A, et al. Multiple microbleeds are related to cerebral network disruptions in patients with early Alzheimer's disease. J Alzheimers Dis 2014;38(1):211–221.

44. Werring DJ, Frazer DW, Coward LJ, et al. Cognitive dysfunction in patients with cerebral microbleeds on T2*-weighted gradient-echo MRI. Brain 2004;127(Pt 10):2265–2275.

45. Fagerholm ED, Hellyer PJ, Scott G, Leech R, Sharp DJ. Disconnection of network hubs and cognitive impairment after traumatic brain injury. Brain 2015;138(Pt 6):1696–1709.

46. Poels MM, Ikram MA, van der Lugt A, et al. Cerebral microbleeds are associated with worse cognitive function: the Rotterdam scan study. Neurology 2012;78(5):326–333.

47. Werring DJ. Cerebral microbleeds: pathophysiology to clinical practice. Cambridge, England: Cambridge University Press, 2011.

48. Yakushiji Y, Nishiyama M, Yakushiji S, et al. Brain microbleeds and global cognitive function in adults without neurological disorder. Stroke 2008;39(12):3323–3328.

49. Qiu C, Cotch MF, Sigurdsson S, et al. Cerebral microbleeds, retinopathy, and dementia: the AGES-Reykjavik Study. Neurology 2010;75(24):2221–2228.

50. Miwa K, Tanaka M, Okazaki S, et al. Multiple or mixed cerebral microbleeds and dementia in patients with vascular risk factors. Neurology 2014;83(7):646–653.

51. Chiang GC, Cruz Hernandez JC, Kantarci K, Jack CR Jr, Weiner MW; Alzheimer's Disease Neuroimaging Initiative. Cerebral microbleeds, CSF p-tau, and cognitive decline: significance of anatomic distribution. AJNR Am J Neuroradiol 2015;36(9):1635–1641.

52. Barnaure I, Montandon ML, Rodriguez C, et al. Clinicoradiologic correlations of cerebral microbleeds in advanced age. AJNR Am J Neuroradiol 2017;38(1):39–45.

53. Ding J, Sigurdsson S, Garcia M, et al. Risk factors associated with incident cerebral microbleeds according to location in older people: the Age, Gene/Environment Susceptibility (AGES)-Reykjavik Study. JAMA Neurol 2015;72(6):682–688.

54. Goos JD, Henneman WJ, Sluimer JD, et al. Incidence of cerebral microbleeds: a longitudinal study in a memory clinic population. Neurology 2010;74(24):1954–1960.

55. Romero JR, Preis SR, Beiser A, et al. Risk factors, stroke prevention treatments, and prevalence of cerebral microbleeds in the Framingham Heart Study. Stroke 2014;45(5):1492–1494.

56. Poels MM, Vernooij MW, Ikram MA, et al. Prevalence and risk factors of cerebral microbleeds: an update of the Rotterdam scan study. Stroke 2010;41(10 Suppl):S103–S106.

57. Sveinbjornsdottir S, Sigurdsson S, Aspelund T, et al. Cerebral microbleeds in the population based AGES-Reykjavik study: prevalence and location. J Neurol Neurosurg Psychiatry 2008;79(9):1002–1006.

58. Akoudad S, Portegies ML, Koudstaal PJ, et al. Cerebral microbleeds are associated with an increased risk of stroke: the Rotterdam study. Circulation 2015;132(6):509–516.

59. Yates PA, Villemagne VL, Ellis KA, Desmond PM, Masters CL, Rowe CC. Cerebral microbleeds: a review of clinical, genetic, and neuroimaging associations. Front Neurol 2014;4:205.

60. Kövari E, Charidimou A, Herrmann FR, Giannakopoulos P, Bouras C, Gold G. No neuropathological evidence for a direct topographical relation between microbleeds and cerebral amyloid angiopathy. Acta Neuropathol Commun 2015;3(1):49.

61. Fisher M, French S, Ji P, Kim RC. Cerebral microbleeds in the elderly: a pathological analysis. Stroke 2010;41(12):2782–2785.

62. Tanskanen M, Mäkelä M, Myllykangas L, Rastas S, Sulkava R, Paetau A. Intracerebral hemorrhage in the oldest old: a population-based study (Vantaa 85+). Front Neurol 2012;3:103.

63. Vernooij MW, van der Lugt A, Ikram MA, et al. Prevalence and risk factors of cerebral microbleeds: the Rotterdam scan study. Neurology 2008;70(14):1208–1214.

64. Mesker DJ, Poels MM, Ikram MA, et al. Lobar distribution of cerebral microbleeds: the Rotterdam scan study. Arch Neurol 2011;68(5):656–659.

65. Pettersen JA, Sathiyamoorthy G, Gao FQ, et al. Microbleed topography, leukoaraiosis, and cognition in probable Alzheimer disease from the Sunnybrook dementia study. Arch Neurol 2008;65(6):790–795.

66. Loehrer E, Ikram MA, Akoudad S, et al. Apolipoprotein E genotype influences spatial distribution of cerebral microbleeds. Neurobiol Aging 2014;35(4):899–905.

67. Schmidt R, Berghold A, Jokinen H, et al. White matter lesion progression in LADIS: frequency, clinical effects, and sample size calculations. Stroke 2012;43(10):2643–2647.

68. Del Brutto VJ, Zambrano M, Mera RM, Del Brutto OH. Population-based study of cerebral microbleeds in stroke-free older adults living in rural Ecuador: the Atahualpa project. Stroke 2015;46(7):1984–1986.

69. Viswanathan A, Greenberg SM. Cerebral amyloid angiopathy in the elderly. Ann Neurol 2011;70(6):871–880.

70. Zonneveld HI, Goos JD, Wattjes MP, et al. Prevalence of cortical superficial siderosis in a memory clinic population. Neurology 2014;82(8):698–704.

71. Charidimou A, Linn J, Vernooij MW, et al. Cortical superficial siderosis: detection and clinical significance in cerebral amyloid angiopathy and related conditions. Brain 2015;138(Pt 8):2126–2139.

72. Gold G, Giannakopoulos P, Herrmann FR, Bouras C, Kövari E. Identification of Alzheimer and vascular lesion thresholds for mixed dementia. Brain 2007;130(Pt 11): 2830–2836.

73. Knudsen KA, Rosand J, Karluk D, Greenberg SM. Clinical diagnosis of cerebral amyloid angiopathy: validation of the Boston criteria. Neurology 2001;56(4):537–539.

74. Goos JD, Kester MI, Barkhof F, et al. Patients with Alzheimer disease with multiple microbleeds: relation with cerebrospinal fluid biomarkers and cognition. Stroke 2009;40(11):3455–3460.

75. Scheid R, Preul C, Gruber O, Wiggins C, von Cramon DY. Diffuse axonal injury associated with chronic traumatic brain injury: evidence from T2*-weighted gradient-echo imaging at 3 T. AJNR Am J Neuroradiol 2003;24(6):1049–1056.

76. Imaizumi T, Miyata K, Inamura S, Kohama I, Nyon KS, Nomura T. The difference in location between traumatic cerebral microbleeds and microangiopathic microbleeds associated with stroke. J Neuroimaging 2011;21(4):359–364.

77. Wang X, Wei XE, Li MH, et al. Microbleeds on susceptibility-weighted MRI in depressive and non-depressive patients after mild traumatic brain injury. Neurol Sci 2014;35(10):1533–1539.

78. Huang YL, Kuo YS, Tseng YC, Chen DY, Chiu WT, Chen CJ. Susceptibility-weighted MRI in mild traumatic brain injury. Neurology 2015;84(6):580–585.

79. Provenzale JM. Imaging of traumatic brain injury: a review of the recent medical literature. AJR Am J Roentgenol 2010;194(1):16–19.

80. Toth A, Kovacs N, Tamas V, et al. Microbleeds may expand acutely after traumatic brain injury. Neurosci Lett 2016;617:207–212.

81. Watanabe J, Maruya J, Kanemaru Y, Miyauchi T, Nishimaki K. Transient disappearance of microbleeds in the subacute period based on T2*-weighted gradient echo imaging in traumatic brain injury. Acta Neurochir (Wien) 2016;158(7):1247–1250.

82. Passos J, Nzwalo H, Valente M, et al. Microbleeds and cavernomas after radiotherapy for paediatric primary brain tumours. J Neurol Sci 2017;372:413–416.

83. Roddy E, Sear K, Felton E, et al. Presence of cerebral microbleeds is associated with worse executive function in pediatric brain tumor survivors. Neuro Oncol 2016;18(11):1548–1558.

84. Tanino T, Kanasaki Y, Tahara T, et al. Radiation-induced microbleeds after cranial irradiation: evaluation by phase-sensitive magnetic resonance imaging with 3.0 tesla. Yonago Acta Med 2013;56(1):7–12.

85. Lupo JM, Chuang CF, Chang SM, et al. 7-Tesla susceptibility-weighted imaging to assess the effects of radiotherapy on normal-appearing brain in patients with glioma. Int J Radiat Oncol Biol Phys 2012;82(3):e493–e500.

86. Lupo JM, Molinaro AM, Essock-Burns E, et al. The effects of anti-angiogenic therapy on the formation of radiation-induced microbleeds in normal brain tissue of patients with glioma. Neuro Oncol 2016;18(1):87–95.

87. Zabramski JM, Wascher TM, Spetzler RF, et al. The natural history of familial cavernous malformations: results of an ongoing study. J Neurosurg 1994;80(3):422–432.

88. Yoon PH, Kim DI, Jeon P, et al. Cerebral cavernous malformations: serial magnetic resonance imaging findings in patients with and without gamma knife surgery. Neurol Med Chir (Tokyo) 1998;38(Suppl):255–261.

89. de Souza JM, Domingues RC, Cruz LC Jr, Domingues FS, Iasbeck T, Gasparetto EL. Susceptibility-weighted imaging for the evaluation of patients with familial cerebral cavernous malformations: a comparison with T2-weighted fast spin-echo and gradient-echo sequences. AJNR Am J Neuroradiol 2008;29(1):154–158.

90. Duval X, Iung B, Klein I, et al. Effect of early cerebral magnetic resonance imaging on clinical decisions in infective endocarditis: a prospective study. Ann Intern Med 2010;152(8):497–504, W175.

91. Champey J, Pavese P, Bouvaist H, Kastler A, Krainik A, Francois P. Value of brain MRI in infective endocarditis: a narrative literature review. Eur J Clin Microbiol Infect Dis 2016;35(2):159–168.

92. Liebeskind DS, Sanossian N, Sapo ML, Saver JL. Cerebral microbleeds after use of extracorporeal membrane oxygenation in children. J Neuroimaging 2013;23(1):75–78.

93. Corrêa DG, Cruz Júnior LC, Bahia PR, Gasparetto EL. Intracerebral microbleeds in sepsis: susceptibility-weighted MR imaging findings. Arq Neuropsiquiatr 2012;70(11): 903–904.

94. Goulenok T, Klein I, Mazighi M, et al. Infective endocarditis with symptomatic cerebral complications: contribution of cerebral magnetic resonance imaging. Cerebrovasc Dis 2013;35(4):327–336.

95. Godechal Q, Mignion L, Karroum O, et al. Influence of paramagnetic melanin on the MRI contrast in melanoma: a combined high-field (11.7 T) MRI and EPR study. Contrast Media Mol Imaging 2014;9(2):154–160.

96. Gaviani P, Mullins ME, Braga TA, et al. Improved detection of metastatic melanoma by T2*-weighted imaging. AJNR Am J Neuroradiol 2006;27(3):605–608.

97. Viswanathan A, Guichard JP, Gschwendtner A, et al. Blood pressure and haemoglobin A1c are associated with microhaemorrhage in CADASIL: a two-centre cohort study. Brain 2006;129(Pt 9):2375–2383.

98. Banerjee G, Kim HJ, Fox Z, et al. MRI-visible perivascular space location distinguishes Alzheimer's disease from subcortical vascular cognitive impairment independently of amyloid burden. European Stroke Journal 2016;1(1 Suppl):613– 780.

99. Kono Y, Wakabayashi T, Kobayashi M, et al. Characteristics of cerebral microbleeds in patients with Fabry disease. J Stroke Cerebrovasc Dis 2016;25(6):1320–1325.

100. Wenz H, Wenz R, Maros M, et al. Incidence, locations, and longitudinal course of cerebral microbleeds in European moyamoya. Stroke 2017;48(2):307–313.

101. Jeon SB, Lee JW, Kim SJ, et al. New cerebral lesions on T2*-weighted gradient-echo imaging after cardiac valve surgery. Cerebrovasc Dis 2010;30(2):194–199.

102. Wilson D, Charidimou A, Ambler G, et al. Recurrent stroke risk and cerebral microbleed burden in ischemic stroke and TIA: a meta-analysis. Neurology 2016;87(14):1501–1510.

103. Poon MT, Fonville AF, Al-Shahi Salman R. Long-term prognosis after intracerebral haemorrhage: systematic review and meta-

analysis. J Neurol Neurosurg Psychiatry 2014;85(6):660–667.

104. Charidimou A, Peeters AP, Jäger R, et al. Cortical superficial siderosis and intracerebral hemorrhage risk in cerebral amyloid angiopathy. Neurology 2013;81(19):1666–1673.

105. Charidimou A, Shakeshaft C, Werring DJ. Cerebral microbleeds on magnetic resonance imaging and anticoagulant-associated intracerebral hemorrhage risk. Front Neurol 2012;3:133.

106. Wang DN, Hou XW, Yang BW, Lin Y, Shi JP, Wang N. Quantity of cerebral microbleeds, antiplatelet therapy, and intracerebral hemorrhage outcomes: a systematic review and meta-analysis. J Stroke Cerebrovasc Dis 2015;24(12):2728–2737.

107. Lovelock CE, Cordonnier C, Naka H, et al. Antithrombotic drug use, cerebral microbleeds, and intracerebral hemorrhage: a systematic review of published and unpublished studies. Stroke 2010;41(6):1222–1228.

108. Wilson D, Werring DJ. Antithrombotic therapy in patients with cerebral microbleeds. Curr Opin Neurol 2017;30(1):38–47.